Rock Mechanics Advances for Underground Construction in Civil Engineering and Mining

Peter K. Kaiser (Centre for Excellence in Mining Innovation, Canada)
Bo-Hyun Kim (Geomechanics Research Centre at MIRARCO, Canada)

Abstract

The underground construction and mining are facing many geomechanics challenges stemming from, geological complexities and stress-driven rock mass degradation processes. Brittle failing rock at depth poses unique problems as stress-driven failure processes often dominate the tunnel behaviour. Such failure processes can lead to shallow unravelling or strainbursting modes of instability that cause difficult conditions for tunnel contractors. This keynote address focuses on the challenge of anticipating the actual behaviour of brittle rocks in laboratory testing, for empirical rock mass strength estimation, and by back-analysis of field observations. This paper summarizes lessons learned during the construction of deep Alpine tunnels and highlights implications that are of practical importance with respect to constructability. It builds on a recent presentation made at the 1st Southern Hemisphere International Rock Mechanics Symposium held in Perth, Australia, in September this year, and includes results from recent developments.

1. Introduction

This paper draws on experiences from major, mostly deep, mining projects and from large, deep tunnelling operations. The author's experience with brittle failing rock in deep mining, underground construction, and Alpine tunnelling was previously presented in keynote lectures: at GeoEng 2000 (Kaiser et al., 2000), summarizing a decade of collaborative research work on brittle rock failure; at the Rockburst and Seismicity in Mines Symposium (Kaiser et al., 2005), introducing new means of complex data interpretation in seismically active mines; at GEAT'05 (Kaiser, 2006), focusing on experiences from deep Alpine tunnelling; at the Asian Rock Mechanics Symposium, highlighting the impact on constructability (Kaiser, 2006); and expands on aspects covered at the Canada–U.S. Rock Mechanics Symposium (Kaiser, 2007) and the 1st Southern Hemisphere International Rock Mechanics Symposium (Kaiser and Kim, 2008). Recent developments and implications of practical importance are highlighted, particularly with respect to the selection of strength parameters for the design of underground excavations in highly stressed rock.

When building in highly stressed rock, instability is imminent and careful engineering with a sound understanding of the rock behaviour is of critical importance for risk management and sound engineering.

In the following, some lessons learned in recent years are reviewed from a geomechanics perspective to facilitate future problem solving and to identify opportunities for improved rock excavation techniques, support design and other ground control measures. By interpreting observed rock failure processes, by explaining factors affecting constructability, and by questioning some well established principles (e.g. commonly used failure criteria), deficiencies in our current state of knowledge can be identified and overcome.

2. Anticipating the rock behaviour

The first principle in understanding rock behaviour is to carefully observe and then interpret field evidence. In this manner, it was found that spalling often dominates over shear failure and that this process is highly dependent on rock confinement (Kaiser and Kim, 2008). It should therefore be anticipated that the strength and bulking behaviour near excavation surfaces (open pit or underground) should differ from those encountered at some distance from an excavation. It also follows that

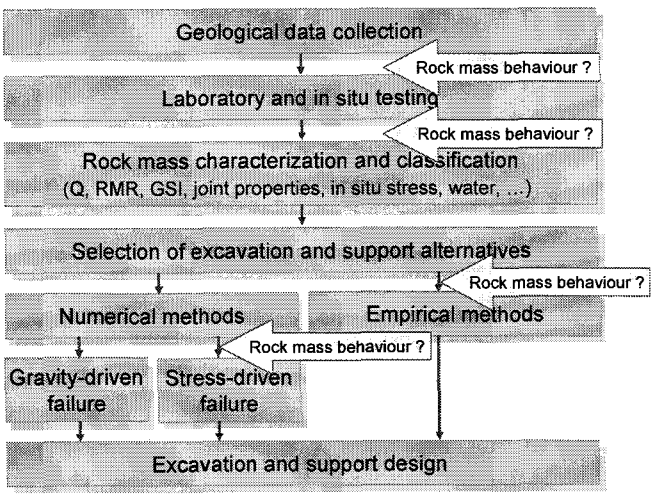

Figure 1 Site characterization approach for standard geo-engineering projects; highlighted are where a sound understanding of rock mass behaviour is needed

fractured rock loses its self-supporting capacity and thus must be more difficult to control during construction (Kaiser, 2006 & 2007; Kaiser and Kim, 2008). This paper build on the previous keynote lectures and expands the concept of s-shaped failure criteria from intact rock to rock mass behaviour.

If brittle rock failure behaviour is not anticipated, e.g., when going deeper or when entering highly stressed ground, rock may behave in an unexpected manner, good "old" ground may become bad ground, and proven technologies may fail to perform well. The geotechnical engineer is thus challenged to anticipate changing rock behaviour modes and to design control measures in such a manner as to facilitate ease of construction. For this reason, three main elements of underground construction are discussed here: (1) the relevance and consequences of brittle failure processes in underground engineering and construction; (2) challenges in anticipating the rock or rock mass strength when brittle failure processes affect or dominate the failure modes of underground excavations, and (3) the consequences for stability assessment on underground constructions.

2.1 Rock behaviour characterization

Site or rock characterization generally follows a well established path (Figure 1) from Geological model to Rock Mass model development, whereby the spatial distributions of rock types as well as rock and rock mass properties and characteristics are characterized and classified. It is however not sufficient to just provide a geological and a rock mass model; it is necessary to translate the knowledge gained from Geological to Rock Mass and then to Rock Behaviour models. Most tender documents elaborate much on the geological and rock mass model but fall short of providing proper descriptions of the rock mass behaviour models. In Figure 1, the arrows indicate where it is necessary to consider anticipated rock behaviour models during the site characterization process.

In underground construction, commonly recognized behaviour modes include wedge failure, squeezing, swelling, etc., and these are reflected in respective modelling tools (UDEC, 3DEC, Unwedge, FLAC, Phases, etc.). Almost exclusively, the most commonly recognized behaviour modes are related to shear failure, either along block boundaries or through the rock mass (elements 1,1 to 1,3 and 3,3 in the tunnel behaviour matrix presented in Figure 2). The effects of tensile failure or spalling are rarely anticipated and correctly modelled, even though they often dominate the degradation process near

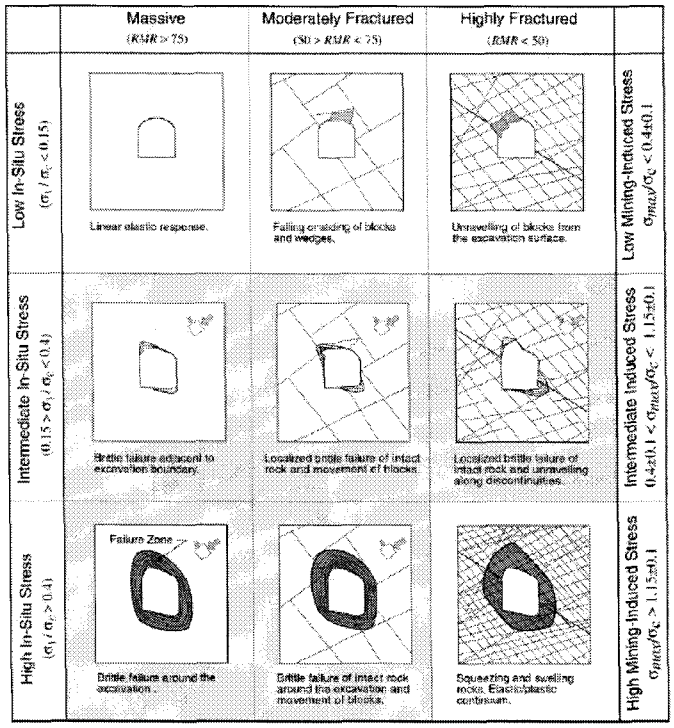

Figure 2 Tunnel failure modes (Kaiser *et al.*, 2000)

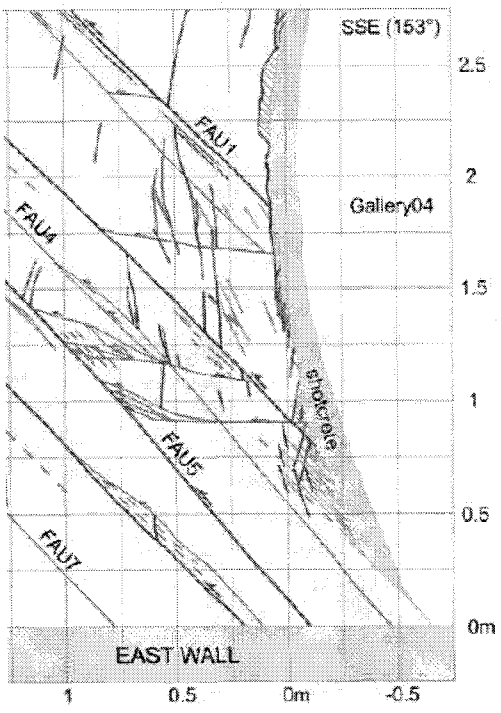

Figure 3 Brittle fracturing near tunnel in Opalinus Clay (Yong *et al.*, 2008)

excavations and negatively affects constructability issues such as stand-up time.

Brittle, tensile rather than shear, failure modes play a role at intermediate to high stress levels and in massive to moderately jointed rock masses (elements 2,1 to 2,3 and 3,1 to 3,2 in tunnel behaviour matrix of Figure 2). Brittle rock behaviour near excavations is more wide spread than commonly anticipated. For example, over-consolidated clays like the Opalinus Clay at Mt. Terri (Yong et al., 2007) show clear signs of tensile failure (Figure 3). Many weaker rock types such as lightly cemented sandstones, Kimberlite, clay shale, etc., do often fail in a brittle manner when lightly confined.

2.2 Brittle failure characteristics

Difficulties in designing underground excavations are often experienced because constitutive laws in numerical models do not necessarily reflect the actual behaviour of the rock. This is particularly true when the fundamental paradigm of the Coulomb yield criteria $\tau = c + \sigma_n \tan \phi$, relating the shear strength τ to a strain-independent cohesion c and a simultaneously acting frictional resistance $(\sigma_n \tan \phi)$, is not valid (Martin, 1997; Martin *et al.*, 1999; Kaiser *et al.*, 2000). As intact rock is strained, cohesive bonds fail first and damage accumulates (Diederichs, 2003). The propagation of tensile fractures depends on the level of confinement (Hoek (1968); used to explain brittle failure by collaborating researchers in Kaiser *et al.* (2000)). Figure 4(a) illustrates that an s-shaped criteria is required to properly describe the entire failure envelope from low confinement with spalling to high confinement shear failure. The existence of this s-shaped failure envelope for many rock types is further examined and verified in this paper.

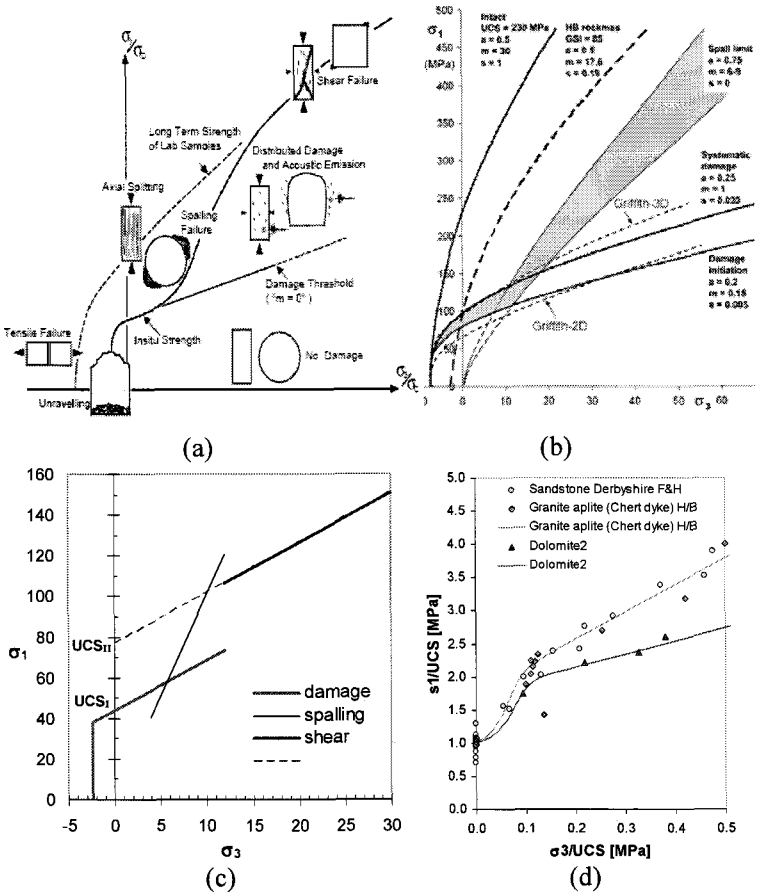

Figure 4 (a) S-shaped failure criteria showing damage threshold, spalling limit and rock mass strength envelope (Kaiser et al. (2000); Diederichs (2003)); (b) bi-nonlinear approximation by Diederichs et al. (2007) for damage threshold and spalling limit; (c) tri-linear failure envelope used for examples presented here; (d) s-shaped failure criteria fitted to data from Sandstone, Granite and Dolomite

A bi-linear or bi-nonlinear criterion is required to capture this dependence on confinement in the low confinement range (near excavations) for rock that is prone to spalling (Figure 4(b)). However, when the confinement is sufficient to prevent spalling, shear failure processes take over and a flatter "shear failure" envelop is reached (Figure 4(c)). For intact rocks (Figure 4(d)) as well as for rock masses (Figure 4(a)), the failure envelop therefore is s-shaped. In the following, the practical relevance of an s-shaped envelope, reaching into the high confinement range, is discussed first by use of a tri-linear failure envelope approximation (Figure 4(c)) with a tension cut-off. This envelope consists of a damage limit through the rock's unconfined compressive strength USC_I (lab test), a spalling limit with slope k_s, and a shear limit with an intercept or apparent unconfined compressive strength UCS_{II}.

For the tri-linear envelope of Figure 4(c), the spalling limit is reached at about 5 MPa (in the middle of the contour range shown in Figure 5) and the shear failure envelope is reached at about 10 MPa (at the outer range of the contours shown in the same figure). In other words, as indicated on Figure 5, there is an "inner shell" where spalling dominates (in this case for $\sigma_3 < 5$ to 8 MPa or < 0.1 to 0.15 UCS_I) and an "outer shell" (at > 0.1 to 0.15 UCS_I) where shear failure dominates.

This separation of behaviour mode has long been recognized in deep South African mines where shear failure is detected far ahead of the advancing face and spalling-type failure near a stope (Spottiswoode et al. (2008) and pers.com.; Ortlepp (1997)).

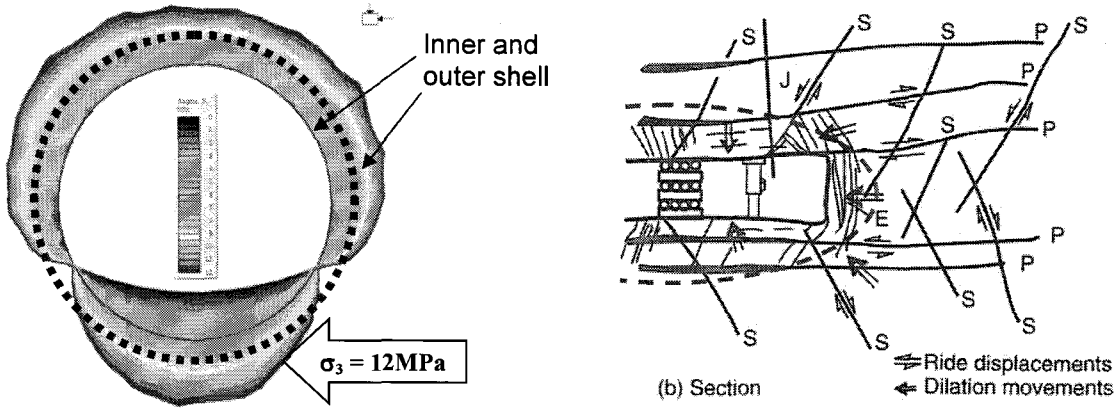

Figure 5 (a) Minor principal stress contours (range 0 - 12 MPa) around excavation in elastic rock for K_o = 0.75; (b) inner shell with spalling and outer shell with shear failure (pers. com. Spottiswoode et al. 2008)

3. Consequences of brittle failure of excavations and pillars

3.1 Strength development near excavations

Contrary to the tangential or major principal stress near an underground excavation, the radial or confinement stress zone (σ_3) is nearly parallel to the excavation geometry as illustrated by Figure 5.

The rapid development of σ_3 in the wall results in a rapid strength development as illustrated by Figure 6 for the wall of the tunnel. Since the σ_3-contours are essentially parallel to the tunnel boundary, nearly identical strength developments occur in the roof as in the walls.

Due to the tri-linear or s-shape of the failure envelope, the rock strength is relatively low near the excavation and increases rapidly to about double strength at a depth of about 1.3m for this case. The tangential stress σ_1 for K_o = 1.33 is also shown in Figure 6 for the roof and walls. Due to the flat, reduced strength near the wall, the tangential stress exceeds the strength not just in the roof (where it would be anticipated for K_o = 1.33) but also in the walls. Field evidence supports this finding (Kaiser 2007).

For support design and support selection, to manage brittle rock failure, it is therefore necessary to identify the rock strength near the excavation (in the inner shell) and this can be approximated by a bi-linear or bi-nonlinear envelope (Diederichs, 2003; Diederichs *et al.*, 2007). For pillar stability assessment, an outer shell problem as discussed below, however, it is necessary to consider all three parts of the s-shaped curve, including the shear failure branch.

In the floor of excavations, the strength increases less rapidly, promoting deeper tensile fracturing and spalling than near curved walls and roof. This has several practical consequences. Some of them are described next.

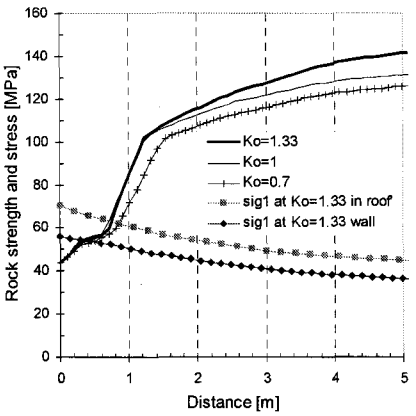

Figure 6 Rock strength development for three stress rations K_0 near excavation wall for tri-linear criteria of Figure 4(c)

3.2 Swelling and slaking potential enhancement by brittle failure

Once the damage and spalling thresholds are exceeded, the volumetric deformation characteristic of brittle failing rock changes drastically as tensile fractures tend to open fractures, and geometric incompatibilities between rock fragments lead to high radial dilation (bulking; Kaiser, 2006). As a consequence, water access to the rock is facilitated through stress

fractures. This supply of water to rock fragments enhances the swell or slaking potential (Kaiser and Kim, 2008).

Brittle failure processes during tunnel advance may therefore play a significant role in rocks where rock degradation processes are facilitated by water ingress. For example, brittle fracturing may enhance the swelling potential and swelling rates in preconditioned or stress damaged zones, e.g., below flat floors (Einstein, 1996) or below insufficiently curved inverts.

In rocks that are prone to slaking (softening and weakening due to water ingress), brittle failure processes can lead to preferential water access paths and thus to non-uniform slaking. In Kimberlites, for example, it is often observed that initially stable tunnels start to squeeze after some time. Tensile fracturing again can provide preferred access paths for water and thus locally enhanced slaking potential.

Recent advances in modelling techniques involving fracture propagation (e.g., ELFEN™) and models permitting combined failure modes involving discontinuities and intact rock (e.g., SRM, synthetic rock mass model) will eventually facilitate the proper simulation of combined shear and tensile failure processes. For the time being however, much can be achieved by recognizing the impact of the s-shaped failure envelope on excavation behaviour and by approximating it by a bi-(non)linear envelope for support design (in the inner shell) and by a tri-linear envelope for aspects involving confined rock (in the outer shell: pillars, etc.).

3.3 Strength development in brittle failing pillars

As indicated above, for pillar stability assessment, it is necessary to consider all three parts of the s-shaped curve (Figure 4) if the confinement inside the pillar exceeds the threshold σ_3 –value at the intersection of the spalling limit with the shear failure envelope (about σ_3 = 10 MPa or σ_3/UCS = 0.1 for case shown in Figure 4(c and d)). Martin and Maybee (2000) used brittle Hoek and Brown parameters (Martin *et al.* 1999) to demonstrate that the pillar strength, contrary to the "best"-fit curves presented by many Figure 7, should non-linearly increases (with an upward rather than a downward curvature) as the pillar width to height ratio (W/H) increases. The authors justified this by the fact that spalling or hour-glassing weakens narrow pillars more than wide pillars. Their interpretation also makes intuitive sense as wide pillars should approach the strength of the confined rock mass, which should be much higher than suggested by the horizontal asymptotic value of about 0.7 to 0.8 UCS_I (Figure 7).

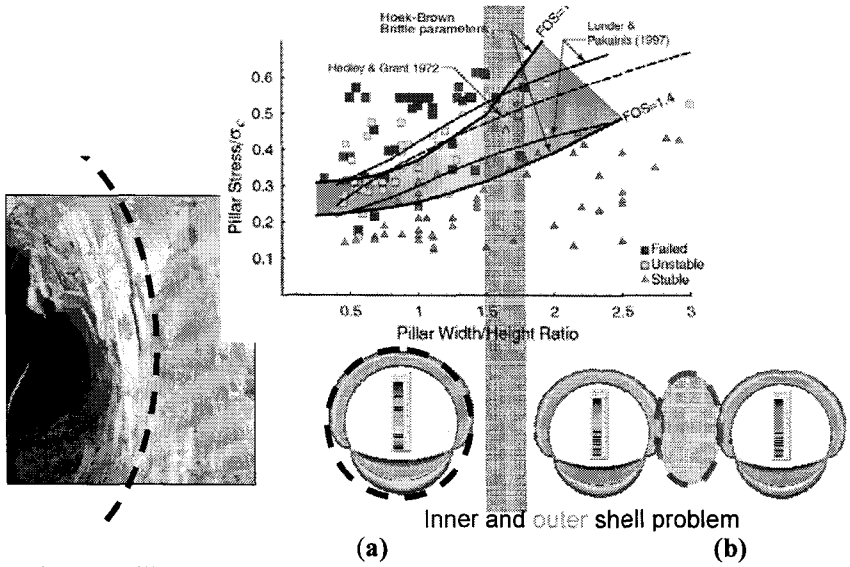

Figure 7 Pillar stability – an inner/outer shell problem: (a) Narrow pillars fail if inner shells join or overlap; and (b) wide pillars (W/H > 1.5 to 1.8) tend to be stable with stable core (inserted chart: Martin and Maybee (2000))

It follows that the strength of wide pillars is strongly influenced by the confined strength of the rock mass and thus by the third leg (the shear strength) of the s-shaped envelope. As illustrated by Figure 7, narrow pillars (W/H< about 1.5) are dominated by inner shell behaviour (leading to hour-glassing; indicated as "failed" by red squares and as illustrated by the photo), while wider pillars are significantly stronger due to the rapid increase in strength in the core (in the outer shell).

3.4 Rock support considerations for brittle failing rock

As illustrated by Figure 5, a low confinement zone of more or less constant depth exists near an unsupported excavation. Even if the tunnel was supported with a liner providing a radial support pressure (typically between 0 and 1 MPa), a low

confinement zone still would exists. Hence, the damage threshold defines the rock strength near the excavation as shown in Figure 6. However, the strength rapidly increases as soon as the confinement is sufficient to reach the spalling limit (at about 0.7 m depth or ~5 MPa for case shown in Figure 6). For a deep tunnel, tensile fracturing is therefore largely confined to the inner shell and, most importantly, tensile failure induced spalling should be expected all around the tunnel independent of K_o.

Kaiser (2007) illustrated how the rock mass bulks in the stress fractured zone and that bulking is highly dependent on confinement. For typical support pressures of $\leq$ 1 MPa, bulking ranges from 7 to 10% (Kaiser *et al.*, 1996). As a consequence, the radial strains in the inner shell are much larger than predicted by standard constitutive models, and the cumulative displacements or convergence with bulking is also much larger (Kaiser and Kim, 2008).

It follows for support design that the wall strength is defined by the low-confinement strength of the rock mass, i.e, by the first and second leg of the tri-linear failure envelope (the damage and spalling strength), that support needs to be designed to control the bulking and manage the resulting elevated convergences.

Stress-driven rock "fragmentation" in the inner shell creates broken rock with varying fragment size and shape distributions (Kaiser, 2007). This stress-driven degradation transforms a rather stable rock mass (if massive to moderately jointed) to a fractured rock mass with a much reduced stand-up time. From a constructability perspective this implies that it is difficult to retain stability of the inner shell when stress-driven fracturing causes rock degradation. Such rock behaviour has slowed the rate of progress at various tunnelling projects utilizing open TBMs (Kaiser, 2007).

4. Laboratory test data revisited

Based on the above presented consequences of brittle rock failure, it is evident that it is necessary to re-evaluate the shape of constitutive models for use in rock mechanics modelling and design.

Both the Coulomb and the Hoek-Brown criterion assume a steady increase in strength with increasing confinement. More importantly, for both criteria it is implied that cohesive and frictional strength components are simultaneously mobilized. Furthermore, rock mass degradation, e.g., using GSI, does not change the form of the failure envelope, and

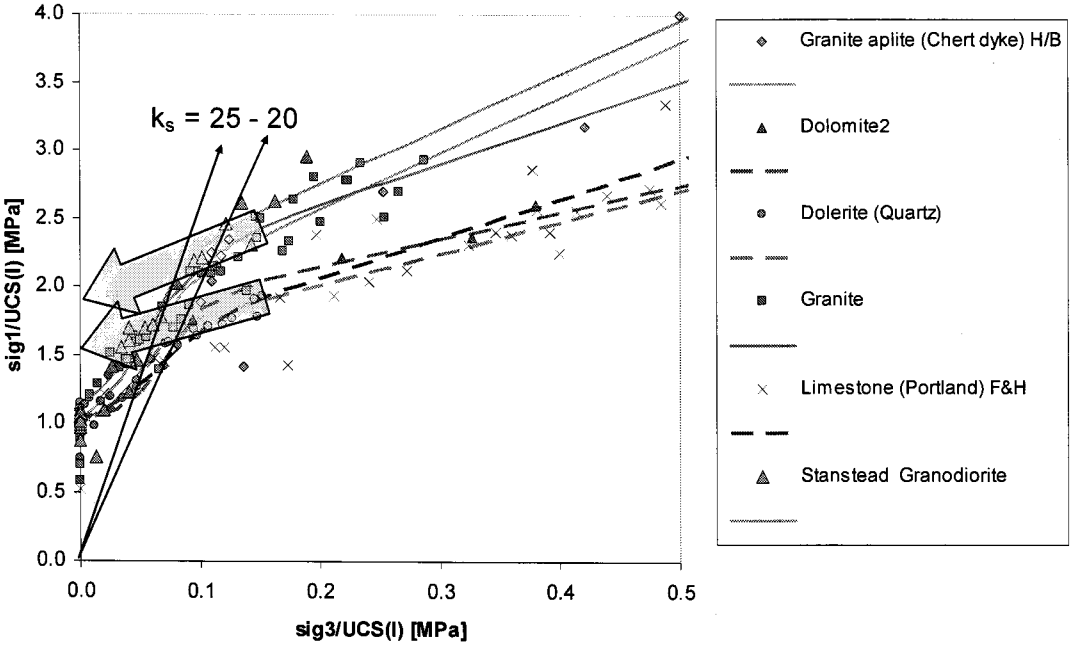

Figure 8 Laboratory test data of two groups with similar behaviour are fitted with s-shaped failure criteria: (a) Granite Aplite, Granite, Granodiorite (apparent UCS_{II} = 1.8 UCS_I; ϕ = 35-37°; k_s = 25; and (b) Dolomite, Dolerite and Limestone (apparent UCS_{II} = 1.55 UCS_I; ϕ = 23-25°; k_s = 20) (data courtesy: E. Hoek and J. Archibault; arrows point at apparent UCS_{II} for two rock types)

various means for residual strength determination (e.g., Cai et al., 2006) do also not alter the shape of the strength envelope.

Ample evidence has been presented in the recent literature by colleagues (primarily Diederichs and Martin) and other researchers that support the bi-linear or bi-nonlinear shape of the failure envelope of rock in the low confinement zone (Figure 4(a & b)). This is now well established based on field observations and extensive back-analyses of cases involving spalling failure.

However, if this process is a fundamental characteristic of brittle failing rock, it should also be observed in laboratory tests. Indeed, when testing hard rocks, it is often observed that samples fail, particularly in unconfined or low confinement tests, by axial splitting, shattering or by progressive spalling. Only at high confinement levels or when a sample contains distinct foliation or weakness planes are shear failure processes observed. Hence, it should be anticipated that brittle rocks might show a similarly tri-linear or s- shaped failure envelop when tested under laboratory conditions.

Kaiser and Kim (2008) revisited Dr. Hoek's data base and showed that the rock strength was typically reduced to the left of a spalling limit of about $\sigma_1/\sigma_3 = 25$ to 20 or typically for $\sigma_3 \leq UCS_I/10$. This is evident from the data and fitted s-shaped failure envelopes shown in Figure 8 for five distinctly different rock types. The strength in the shear failure zone can be described with an apparent unconfined strength, UCS_{II}, of 1.5 to 2- times the standard unconfined compression test strength (UCS_I).

4.1 s-shaped failure criteria for brittle failing intact rock

The s-shaped failure criterion shown in Figure 8 can be described by the following equation:

$$\sigma_1' = k_2\sigma_3' + UCS_{II} + \left[\frac{(UCS_I - UCS_{II})}{1 + e^{(\sigma_3' - \sigma_3^0)/\delta\sigma_3}}\right] \qquad \text{Eqn (1)}$$

where k_2 is gradient at zero confinement (assumed to be the same as in the high confinement range), k_s is the spalling limit (varying with rock type), σ^0_3 and $\delta\sigma_3$ are shape parameters, and UCS_I and UCS_{II} are intercepts at zero confinement (actual and apparent UCS, respectively).

Since most numerical modeling programs do not yet allow for the use of an s-shaped failure criterion, the strength envelope can be approximated by a tri-linear criteria as illustrated in Figure 4(c) or as superimposed on Figure 9(b) for the Quartzite (UCS_I = 140 ±30 MPa; UCS_{II} = 300 ±15 MPa; k_s = 35 to 15 to 10 for intact to structurally controlled breaks).

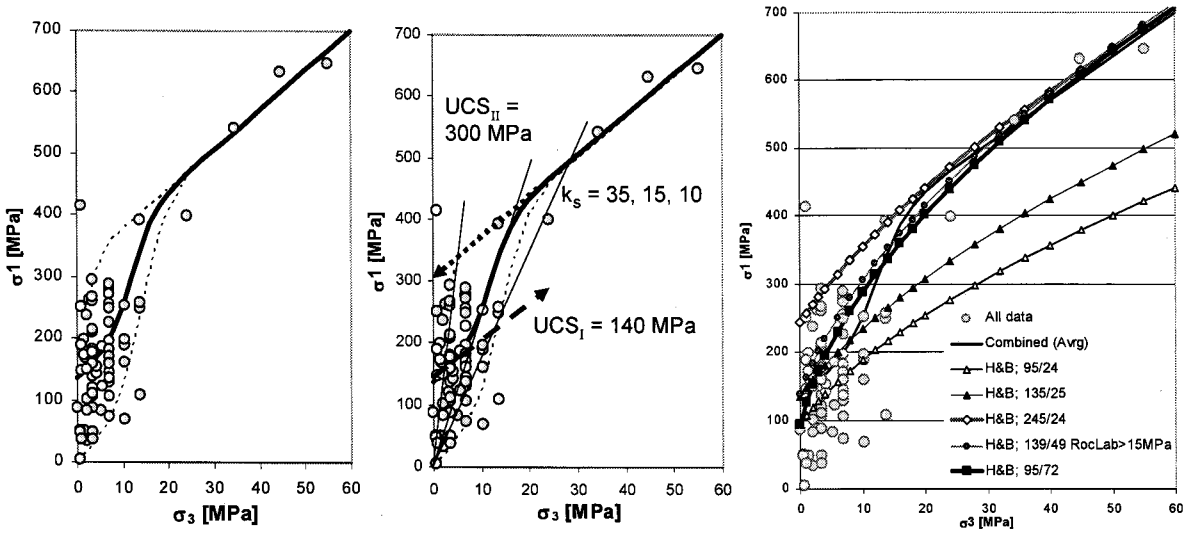

(a) (b) (c)

Figure 9 Data from friable Quartzite: (a) fitted s-curve for all data and upper and lower limit; (b) respective linearized approximations; (c) Hoek and Brown envelopes obtained by various fitting approaches with parameters listed in Table 1 (UCS and m_i values are shown in legend as UCS/ m_i)

From a brief review of published data from igneous, metamorphic and sedimentary rocks, it is found that the UCS ratio (UCS_{II}/UCS_I) typically ranges between 1.5 and 2 with a range of 1.3 to >3. This indicates that most rocks have a brittle failure component.

4.2 Guidelines for design parameter selection for brittle intact rock

It is evident from the above that design parameters for brittle failing rocks must be selected with care and with the design problem in mind. Until an s-shaped failure criterion has been finalized, tested and is ready for use in numerical modelling, constitutive model and failure envelope adopted for support design may have to differ from those used for pillar design (see above). This is illustrated here for the data set shown in Figure 9(a). The average UCS for this rock (data not shown) is 95 MPa for all data and 125 MPa for intact breaks only. Parameters for four approaches to obtain the rock strength are listed in Table 1 and the corresponding non-linear envelopes are shown in Figure 9(c).

The obvious question arises: how to select the most appropriate intact rock strength envelope for this Quartzite? A detailed discussion of parameter selection was presented by Kaiser and Kim (2008) and is reproduced in the following since it is most important that rock strength parameters are selected following an appropriate process.

The m_i -values for approach B and D are clearly out of range based on commonly recommended values and thus would be rejected. However, based on the above presented discussion, an unusually high m_i-value of 72 would clearly overall represent the results from the laboratory testing program best (Figure 9(c))

Table 1 Parameters for Hoek and Brown criteria shown in Figure 9(c)

	Approach	UCS [MPa]	m_i
A	Average from UCS tests and m_i from published rock type tables: $m_i = 23\pm3$ for Quartzite	95 (average)	24 (assumed)
B	RocLab™ (Rocscience) applied to all data	139	50
C	RocLab™ applied to data from samples failing through intact rock	245	24
D	Best fit to all data without RocLab constraint of $m_i \leq 50$ and average UCS	95	72

Approach A and C: Approximation using UCS data from laboratory tests and published mi-values

In mining, modelling is often based on UCS data only and m_i is estimated from recommended property tables (e.g., Hoek, 2007). The resulting failure envelope (Approach A) clearly underestimates the intact rock strength of the Quartzite in the high confinement range (> 10 MPa; Figure 9(c)) if the average UCS were used. On the other hand, if the UCS of only those tests with intact breaks were used (Approach C), then the resulting failure envelope clearly over-estimates the strength of the Quartzite in the low confinement range (<10 MPa; Figure 9(c)).

Approach B and C: Use of RocLab™

When using any fitting procedure to obtain Hoek and Brown parameters, data must cover the confinement range of σ_3 = 0 to UCS/2 (see frequently asked question about determination of m_i on homepage of RocLab™ http://www.rocscience.com). Because of test cell constraints, triaxial test are commonly conducted with confining pressures up to 60 MPa. Consequently, as for the Quartzite shown above, fitting approaches to obtain Hoek and Brown parameters are strictly only applicable for rocks with UCS < 120 MPa and parameters can thus, strictly speaking, not be obtained for hard brittle rocks. Furthermore, RocLab™ limits m_i to 50 and thus cannot be used for rocks with distinct s-shaped failure behaviour.

Obtaining representative Hoek and Brown parameters for rocks with s-shaped failure behaviour

For rocks with distinct s-shaped failure behaviour, a best-fit Hoek and Brown parameter set can be obtained by linear regression in the $(\sigma_1 - \sigma_3)^2/UCS^2$ versus σ_3/UCSspace (Approach D; forcing A linear regression line through (σ_1 –

$\sigma_3)^2/UCS^2 = 1$). However, it must be noted that the corresponding m_i-value ($m_i = 72$ for the Quartzite) are unusually high and that standard approaches to obtain the rock mass strength (e.g., by GSI-based degradation) may not be applicable. Nevertheless, such a fitting approach will lead to a parameter set for the intact rock that is on average representative for the entire confinement range (with high uncertainty in the low confinement range).

Sectional fitting for limited confinement ranges

For rocks with distinct s-shaped failure behaviour, it is therefore more appropriate to consider the confinement range relevant for a given engineering problem before fitting and selecting design parameters. For the Quartzite of Figure 9(c) reproduced Figure 10, the inner zone extends to about $\sigma_3 < 0.1\ UCS_I$ and the outer zone beyond.

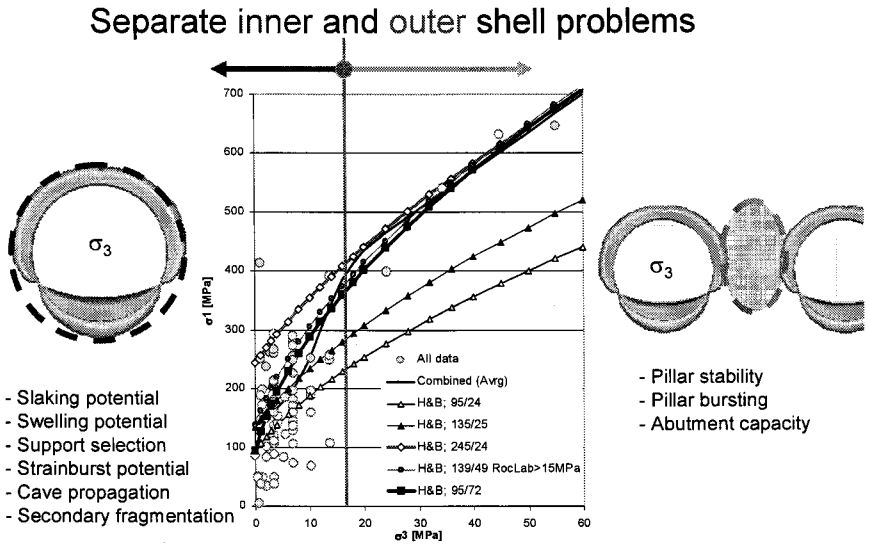

(a) (b) (c)

Figure 10 (a) Illustration and listing of "inner shell" problems; (b) (c) Hoek and Brown envelopes as presented in Figure 9; and (c) illustration and listing of "outer shell" problems

For support design, the rock behaviour near the excavation, in a confinement range of 0 to typically 5 MPa, is most relevant. From Figure 9(c), it follows that the parameter sets (between 95/24 to 139/24, or 120/24 on average with a standard deviation of about 40 MPa on UCS) would be appropriate for the low confinement zone (inner shell). However, a cut-off as recommended by Diederichs *et al.* (2008), or with $k_s = 15$ to 10, would have to be applied to prevent excessive depths of failure predictions.

For pillar design, the rock behaviour in the pillar core, in a typical confinement range of > 5 MPa for mining at depth, is most relevant. From Figure 9(c), it is evident that the parameter sets (245/24) with a standard deviation of about 15 MPa on UCS, would be appropriate for the highly confined zone (outer shell). However, the effect of spalling and hour-glassing is to be predicted by using the parameter set for the inner shell.

This is further highlighted by the division of the stress space into an inner and outer shell (Figure 10). The type of problems that are inner shell problems are listed on the left side (Figure 10(a)) and those that are outer shell problems on the right side (Figure 10(c)).

5. s-shaped failure criteria for brittle failing rock masses

From the previous discussion, it follows that Figure 4(a) needs to be modified to take into account that the intact rock strength is also s-shaped. This is illustrated by the data superimposed on Figure 11.

Procedures to obtain s-shaped failure envelopes for the rock mass corresponding to the s-shaped intact rock strength, following the GSI approach (Figure 12), are under development. If it is assumed that the currently adopted degradation approach to obtain the Hoek and Brown parameters s and m_b for the rock mass is applicable, then it can be applied for each section of the s-curve (the low and the high confinement range) to obtain an s-shaped rock mass envelope. This aspect remains an outstanding challenge for rock engineering in brittle rock masses and will require further research and calibration.

Nevertheless, rock and rock mass strength parameters for brittle failing rock should be established separately for the low and high confinement zones and then applied to zones where spalling or shear failure modes are dominating the rock behaviour (e.g., for inner and outer shell modeling).

The most general form of the Hoek-Brown criterion is given by:

$$\sigma_1 = \sigma_3 + \sigma_c \left(m_b \frac{\sigma_3}{\sigma_c} + s \right)^a \qquad \text{Eqn (2)}$$

where, m_b and a are constants for the rock masss; σ_c is the uniaxial compressive strength of the intact rock; and σ_1 and σ_3 are the axial and confining effective principal stresses, respectively.

This criterion works well for most rocks of good to fair quality, when the rock mass strength is controlled by tightly interlocking angular rock pieces. The failure of such rock masses can be defined by setting a = 0.5 in Equation 2:

$$\sigma_1 = \sigma_3 + \sigma_c \left(m_b \frac{\sigma_3}{\sigma_c} + s \right)^{0.5} \qquad \text{Eqn (3)}$$

For poor quality rock masses in which the tight interlocking has been partially destroyed by shearing or weathering, the rock mass has no tensile strength or cohesion and specimens will fall apart without confinement. For such rock masses s = 0 and a may be a function of rock mass quality (Hoek et al. 1995). When highly confined, the rock mass may though have an apparent cohesion with s > 0 for $\sigma_3 > 0.1\ UCS_I$.

It is practically impossible to carry out triaxial or shear tests on rock masses at a scale appropriate for surface or underground engineering. Numerous attempts have been made to overcome this problem by testing small scale models, made up from assemblages of blocks or elements of rock or of carefully designed model materials. However, our ability to predict the strength of jointed

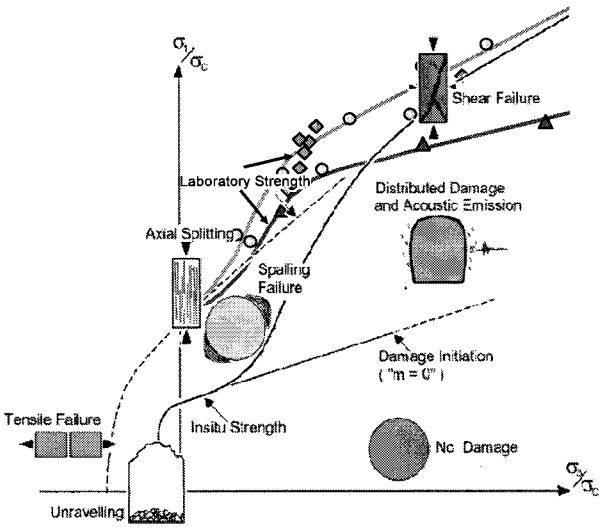

Figure 11 S-shaped failure criteria concept showing modified intact rock strength s-curves (modified after Kaiser *et al.* (2000) or Diederichs (2003))

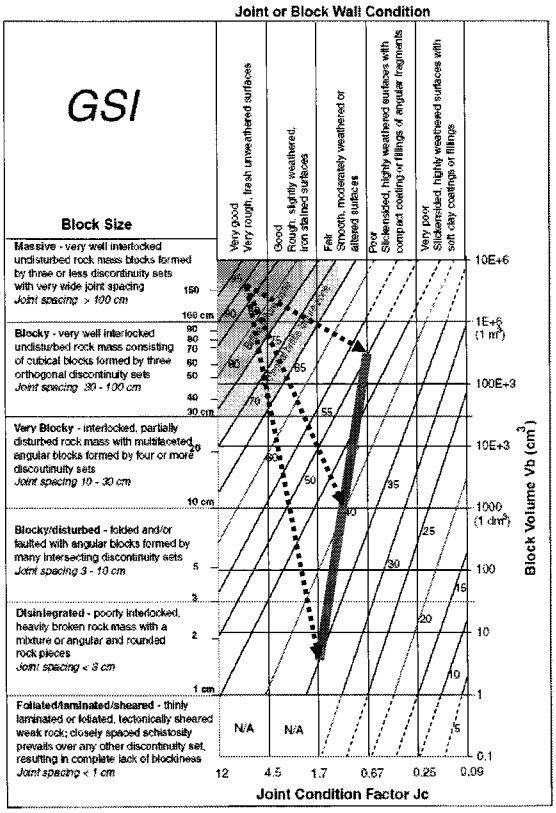

Figure 12 GSI-chart showing degradation paths for various rock types from massive gneiss, to friable quartzite, to massive granite (Kaiser, 2007)

rock masses on the basis of direct tests or of model studies is still severely limited.

For this reason, Equations 2 and 3 are of little practical value unless the values of the material constants m_b and s can be estimated in some manner. Hoek and Brown (1988) suggested that these constants could be estimated from the 1979 version of Bieniawski's Rock Mass Rating (RMR), assuming completely dry conditions and a very favorable joint orientation. While this process is acceptable for rock masses with RMR values of more than about 25, it does not work for very poor rock masses since the minimum value which RMR can assume is 18. In order to overcome this limitation, a new index called the Geological Strength Index (GSI) was introduced (Hoek et al. 1995; Figure 12). The value of GSI ranges from about 10, for extremely poor rock masses, to 100 for massive rock.

The relationships between m_b/m_i and s for a = 0.5 and the Geological Strength Index (*GSI*) according to Hoek et al. (1995) are as follows for 70 > *GSI* > 25 (and undisturbed rock masses):

$$\frac{m_b}{m_i} = \exp\left(\frac{GSI-100}{C_m}\right) \quad \text{with } C_m = 28 \text{ recommended by Hoek et al. (1995)} \qquad \text{Eqn (4)}$$

$$s = \exp\left(\frac{GSI-100}{C_s}\right) \quad \text{with } C_s = 9 \text{ recommended by Hoek et al. (1995)} \qquad \text{Eqn (5)}$$

The constants C_m and C_s characterize the rate of strength loss as a function of rock quality degradation and Hoek et al. (1995) assumed that these parameters are constant over the entire confinement range, i.e., they are assumed to be the same for the inner and outer shell. For brittle rocks, however, it is now understood that the degradation by spalling processes is much more rapid and more significant in the low confinement range (in the inner shell) than at high confinement when shear failure dominates (in the outer shell). Hence, these constants should be a function of confinement $C_s = f(\sigma_3)$ and $C_m = g(\sigma_3)$ or at least should differ for the inner and outer shell. The constants should be higher in the outer shell where spalling and dilation is constrained and some failure though intact rock (rock bridges and asperities) must occur.

The change in degradation rate for s is illustrated by Figure 12; illustrating that the brittle limit of $\sqrt{s}$ = 0.4 (Martin et al. 1999) is reached for GSI = 84 with Cs = 9. Cai et al. (2004) found that brittle behaviour may be encountered in rocks with GSI as low as 65. Thus, C_s = 5 to 15 (on average C_s = 9 as originally proposed) should be applicable for brittle rocks in the inner shell.

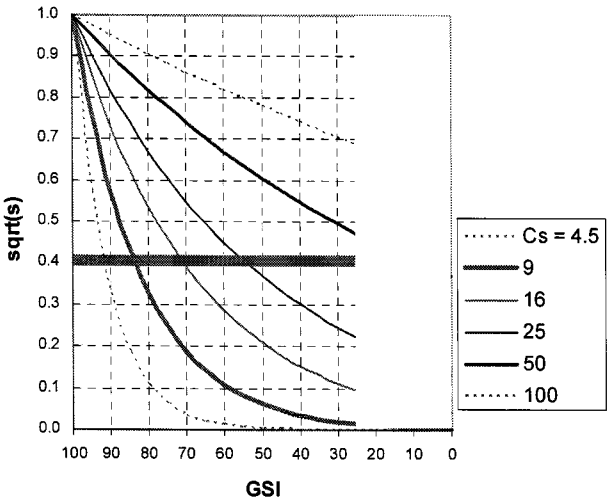

Figure 13 Rate of rock mass degradation $\sqrt{s}$ as a function of GSI for various C_s- constant

Furthermore, it is hypothesized that the rate of degradation in the outer shell is less rapid for several reasons. First, when highly confined rough joints are prevented from dilating, an apparent cohesion is mobilized as shear through asperities must occur. Second, rock bridges, when confined, are stronger (less prone to tensile failure) and thus add an additional apparent cohesion. Consequently, C_s must be higher in the outer shell than in the inner shell or $C_s >> 9$ for highly confined (>0.1 UCS) and very tight rock.

At this stage, it is not yet know how to determine C_s for the outer shell and further research is required. The impact on the failure envelope though is illustrated by the three cases shown in of Figure 14 the Quartzite presented in Figure 9.

In Figure 14(a), only the inner shell properties are degraded with C_s = 9 and the outer shell in not degraded at all ($C_s = \infty$). The scatter in data due to the effect of flaws and weaknesses in the Quartzite in the low confinement zone can be nicely fitted by this GSI-dependent degradation.

In Figure 14(b), the inner shell properties are degraded with C_s = 9 and the outer shell is degraded at a lesser rate with C_s = 50. A GSI of 100 to 70 covers the entire range of laboratory test on small samples with flaws and weaknesses (Figure 14

(b)). If the rock mass would degrade at this rate, the rock mass failure envelop would be s-shaped for the entire applicable GSI range (100 to 25).

In Figure 14(c), the inner shell and outer shell properties are degraded equally at $C_s = 9$. A GSI of 100 to 95 covers the range of laboratory test on small samples with flaws and weaknesses. In this case the s-shaped failure envelope is rapidly lost at about GSI < 80.

As indicated above, further studies and back-analyses of pillars or micro-seismicity near caves will be required to establish guidelines for C_s in the shear failure range. From qualitative observations it is anticipated that C_s may range from 15 to 50 for the outer shell in hard, competent (non-altered) rock masses.

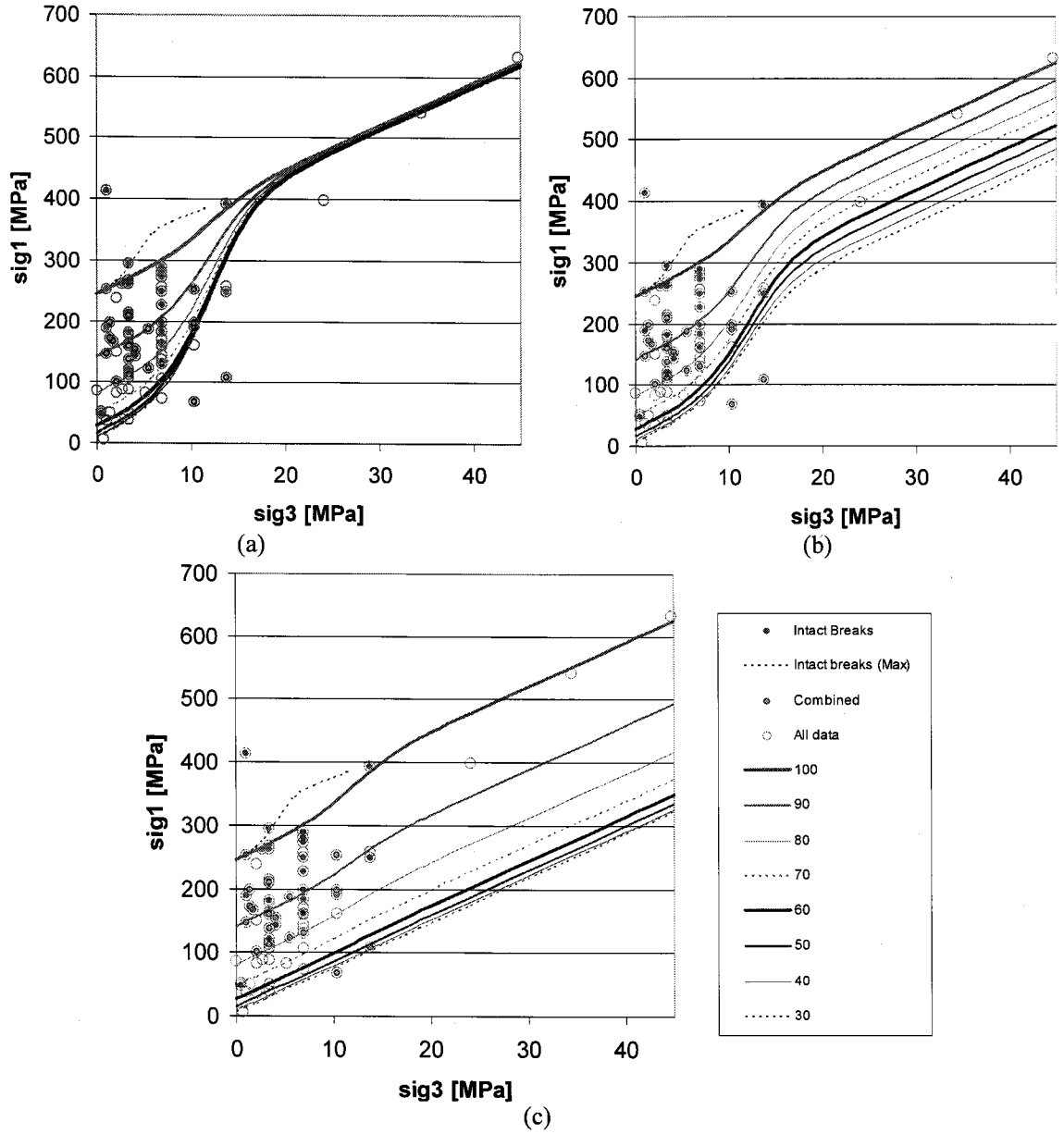

Figure 14 Rate of rock mass degradation $\sqrt{s}$ as a function of GSI for various C_s- constant Figure 15 Three cases of increasing rock mass degradation in the shear failure zone (outer shell): (a) $C_s = 9/\infty$; (b) $C_s = 9/50$; and (c) $C_s = 9/9$

6. Conclusion - Lessons learned

When mining in brittle ground, the rock behaviour can change drastically when progressing to greater depth where the rock mass may be highly confined.

By observing and interpreting brittle rock behaviour, it is now possible to understand and anticipate the rock behaviour such that design and construction procedures can be matched to the ground. At depth, rock becomes brittle and fails at least in part, i.e., near the excavation, by tensile failure processes. This degradation cannot be prevented but must be managed by appropriate rock reinforcement and retention techniques.

Design based on convention failure criteria (Coulomb or Hoek-Brown) may mislead the designers. This is of particular concern when numerical codes with conventional constitutive models and inappropriate strength parameters are adopted. As a consequence, failure may both be over- or under-predicted depending on which part of the s-shaped curve is used to select rock strength parameters.

Due to the distinctly different behaviour in the inner shell, extreme care must be taken when using measurements from the low confinement zone to determine confined rock parameters for the outer shell (e.g., for pillar design). There is a distinct possibility that back-analyses of measurements in the inner shell will significantly underestimate the confined rock mass strength and thus lead, for example, to conservative pillar designs.

With respect to anticipating underground construction difficulties, it is most important to recognize that the rock and rock mass strength near the excavation may be significantly reduced for brittle failing rock (in the inner shell). Hence, spalling, stain-bursting, limited stand-up time of the inner shell, and high potential for overbreak should be anticipated. Equipment (e.g., type of TBM) is to be selected to properly manage these unfavourable rock behaviour modes.

Such processes cannot only occur at the excavation walls or tunnel backs but in the floor and at the tunnel face. The latter may lead to tunnel face instability issues (Kaiser, 2006 and 2007) with related implications for the utilization of TBMs. The former may lead to floor heave or degradation (including slaking and swelling) potential.

In summary, spalling processes must be understood when selecting excavation and support techniques or classes; they must be appropriate to manage broken ground.

Acknowledgements

Some of the studies presented in this article were partially funded by the Natural Sciences and Engineering Research Council of Canada and contributions of former graduate students and long-term research collaborators listed in the quoted references below are thankfully acknowledged. Much practical experience reflected in this paper stems from valuable collaborations with representatives of underground contractors (MATRANS and TAT consortia, Switzerland), TBM manufacturer (Herrenknecht AG, Germany), mining companies (Vale Inco, Goldcorp, Rio Tinto, etc.), and many others. Their contributions and support are thankfully acknowledged.

References

1. Cai, M., Kaiser, P.K., Tasaka, Y., and Minami, M. (2006). Determination of residual strength parameters of jointed rock masses using GSI system. Int. J. of Rock Mech., 44(2): 247-265.
2. Cai, M., P.K. Kaiser, H. Uno, Y., Tasaka, M. Minami and Y. Hibino, 2004.Estimation of rock mass strength and deformation modulus using GSI system – a quantitative approach. International Journal of Rock Mechanics and Mining Sciences, 41(1): 3-19.
3. Diederichs, M.S., Carvalho, J.L. and Carter, T.G. and (2007). A modified approach for prediction of strength and post yield behaviour for high GSI rock masses in strong, brittle ground. , 1st Canada-U.S. Rock Mech. Symp., pp. 249-257.
4. Diederichs, M.S., Kaiser, P.K. and Eberhard, K.E. (2004). Damage initiation and propagation in hard rock and influence of tunnelling induced stress rotation. Int. J. Rock Mech. Min. Sci., 41: 785-812.
5. Diederichs, M.S. (2003). Rock fracture and collapse under low confinement conditions, Rocha Medal Recipient, Rock Mech. Rock Engr., 36(5):339-381.
6. Einstein, H.H. (1996). Tunnelling in difficult Rock – swelling behaviour and identification of swelling rocks. Rock Mechanics and Rock Engineering. 29(3):113-124; see also: Einstein, HH.; Bischoff,, N. und Hofmann E., 1972. Das Verhalten von Stollensohlen in quellendem Mergel. Proc. Symposium Untertagbau, Luzern, pp. 296 – 312.
7. Hoek, E., 2007. Practical rock engineering, 2nd ed. Rocscience Inc.

8. Hoek, E., P.K. Kaiser and W.F. Bawden, 1995. Rock Support for Underground Excavations in Hard Rock. A.A. Balkema, Rotterdam, 215 p.
9. Hoek, E. (1968). Brittle Failure of Rock. In Rock Mechanics and Engineering Practice, John Wiley & Sons Ltd. London, 99-124.
10. Martin, C.D. and Maybee, W.G. (2000). The strength of hard-rock pillars. Int J Rock Mech. and Min. Sc. 37(8):1239-1246.
11. Martin, C.D.. McCreath, D.R. and Maybee W.G. (2000). Design approaches for hard-rock pillars. Proc. 53rd Can. Geot. Conf., Bitech Publishers Ltd., Richmond, (ed. LeBoeuf), 1:291-298.
12. Martin, C.D., Kaiser, P.K. and McCreath, D.R. (1999). Hoek-Brown parameters for predicting the depth of brittle failure around tunnels. Canadian Geotechnical Journal, 36(1):136-151.
13. Kaiser, P.K. and B-H. Kim, 2008. Rock mechanics challenges in underground construction and mining, Keynote lecture, 1st Southern Hemisphere International Rock Mechanics Symposium, Perth, Australia, 1:23-38.
14. Kaiser, P. K. (2007). Rock mechanics challenges and opportunities in underground construction and mining. Keynote lecture, 1st Canada-U.S. Rock Mechanics Symposium, on CD, 47p.
15. Kaiser, P. K. (2006). Rock mechanics consideration for construction of deep tunnel in brittle ground. Keynote lecture, Asia Rock Mechanics Symposium, Singapore, 12 p, on CD.
16. Kaiser, P.K. (2005). Tunnel stability in highly stressed, brittle ground - Rock mechanics considerations for Alpine tunnelling. Geologie und Geotechnik der Basistunnels, Keynote lecture at GEAT'05 Symposium, Zürich, Switzerland, pp. 183-201 (2006).
17. Kaiser, P.K., Diederichs, M.S., Martin, C.D., Sharp, J. and Steiner, W. (2000). Underground works in hard rock tunnelling and mining. GeoEng2000, Technomic Publ. Co., pp. 841-926.
18. Kaiser, P.K., McCreath, D.R. and Tannant, D.D. (1996). Canadian Rockburst Support Handbook, Mining Re-search Directorate, Sudbury, Canada, 314 p.; also Drift support in burst-prone ground. CIM Bulletin, 89(998): 131-138.
19. Ortlepp, W.D. (1997). Rock Fracture and Rockbursts: an illustrative study. Monograph series M9. South African Inst. Min. Metall. 220p.
20. Spottiswoode, S.M., L.M. Linzer and Majiet, S. (2008). Energy and stiffness of mine models and seismicity. 1st Southern Hemisphere International Rock Mechanics Symposium, Perth, Australia, 1:693-707.
21. Yong, S., Kaiser, P.K., Löw, S. and Corrado, F. (2008). The Role of heterogeneity on the development of excavation-induced fractures in the Opalinus Clay, Canadian Geotechnical Conference, Edmonton, 8p (in press).